Nanomed Res J 9(3):228-242, Summer 2024

RESEARCH ARTICLE

Synergistic effect of Ganoderma lucidum Triterpenoids and biosynthesized Zinc Oxide nanoparticles against some dermatophytes

Hasan Jamal Kareem*, Alaa Mohsin Al-Araji

Department of Biology, College of Science, University of Baghdad, Baghdad, Iraq

ARTICLE INFO

Article History:
Received 22 Mar 2024
Accepted 03 May 2024
Published 01 Aug 2024

Keywords:
Ganoderma lucidum
Triterpenoids
Nanoparticles
Zinc oxide
Dermatophytes
Antifungal activity

ABSTRACT

G. lucidum mushroom has been recorded in conventional medicine for more than 2000 years due to has several bioactive compounds including triterpenoids (GLTs). This study aimed to extract and detect of the triterpenoids and biological synthesis of Zinc oxide nanoparticles by using the aqueous extract of this mushroom, then evaluate their antifungal activity against four dermatophytes. From the 1000 g of G. lucidum dried fruiting bodies powder which were used in this study, 16.1 g GLTs was extracted. HPLC was used to analyses GLTs and detection of Ganoderic Acid by using (Ganoderic Acid A) as a standard. The results showed that the concentration of Ganoderic acid in the sample was 985 µg per gram of the extract. ZnO nanoparticles were biosynthesized by using 1 gm of zinc chloride salt with 10 ml of G. lucidum aqueous extract to obtain ZnO nanoparticles. The biosynthesized ZnO nanoparticles were characterize by using different approaches included UV spectrophotometer, FTIR, AFM, EDX, and FESEM. These techniques demonstrated the biosynthesis of ZnO nanoparticles with a diameter 44.62 nm. The result of antifungal activity of these compounds showed significant difference among treatments for inhibit the four dermatophytes. The combinations between GLTs with ZnO nanoparticles showed synergistic effect to inhibit the growth of M. canis, T. rubrum, E. floccosum, and T. mentagrophytes. The concentration 100 mg/ ml of this treatment showed highest inhibition percentage followed by 50 and 25 mg/ml. In other words, the inhibition percentage increased by increasing the concentrations of the tested treatments.

How to cite this article
Jamal Kareem H., Mohsin Al-Araji A. Synergistic effect of Ganoderma lucidum Triterpenoids and biosynthesized Zinc Oxide nanoparticles against some dermatophytes. Nanomed Res J, 2024; 9(3): 228-242. DOI: 10.22034/nmrj.2024.03.001

INTRODUCTION

The medicinal mushroom *Ganoderma lucidum* (*G. lucidum*) belongs to Basidiomycota division characterized by a woody texture, this mushroom found in both tropical and temperate areas across Asia, Europe and North America [1]. *G. lucidum* has been recorded in Chinese conventional medicine for more than 2000 years. The Chinese Pharmacopoeia records the activity of this mushroom in reducing cough and asthma. It additionally recommended for symptoms like anxiety, insomnia, palpitations and lung insufficiency [2]. Several studies indicated that this mushroom has multiple active compounds like triterpenoids, polysaccharides, steroids, sterols, nucleotides, fatty acids, and other substances [3, 4]. Nevertheless, polysaccharides and triterpenoids are recognized as the principal active ingredients that regulate numerous pharmacological actions [5]. *G. lucidum* triterpenoids (GLTs) are a specific type of terpenes which consist of six isoprene units. GLTs have cyclic or linear chemical structures due to the presence of isoprene units. Ganoderic acid is a specific type of GLTs which consist of two linear isoprenes and four cyclic isoprenes. More than one hundred types of ganoderic acid were extracted from this mushroom [6]. The chemical configuration of GLTs originating from lanostane, a substance synthesized from lanosterol via squalene cyclization during biosynthesis [7]. The increasing

* Corresponding Author Email: *hasan.jamal2302@sc.uobaghdad.edu.iq*

rate of microbial diseases together with antimicrobial resistance, has been recognized as a major public health concern, stimulating the discovery of new antimicrobial agents by using of nanotechnology. Nanotechnology offer excellent options in several applications, with metallic nanoparticles identified for their antimicrobial activity [8].

Nanotechnology is a rapidly advancing multidisciplinary scientific area covering physics, chemistry, and biology. Nanotechnology involve the production of tiny particles' information within a restricted region of materials, devices, and measurements. Nano data is obtained through constituent particles called nanoparticles, which consist of molecules and atoms measuring between 1 and 100 nm in size. It is utilized to produce more efficient methodologies in technology, energy conservation, science, medicine, and other fields [9, 10]. Nanoparticles are generate by different methods which include biological, chemical and physical approaches [11]. Among these approaches, the biological or green synthesis recognized as environmentally friendly, cost-effectiveness, and simple procedure. Moreover, the utilization of biological synthesis approach for nanoparticles may improve the properties of these particles by means of the reduced the size and specific shape obtained [12, 13]. Among these nanoparticles, zinc oxide (ZnO) nanoparticles are a class of metal oxide nanoparticles characterized by unique chemical and physical properties, it is an inorganic chemical substance with numerous applications in daily life. The fast growth of nanotechnology in recent years is playing a significant role in the growth of ZnO nanoparticles which display unique features. ZnO nanoparticles improved catalytic properties when their diameters bellow 100 nm due to the significant surface to volume ratio [14]. However, modern studies showed that the *G. lucidum* and zinc oxide nanoparticles have antidermatophytic activity [15, 16].

The dermatophytes are a group of closely related fungi that have the capacity to invade keratinized tissue (skin, hair, and nails) of humans and other animals to produce an infection called dermatophytosis, commonly referred to as ringworm. Infection is generally cutaneous and restricted to the nonliving cornified layers because of the inability of the fungi to penetrate the deeper tissues or organs of immunocompetent hosts [17]. Dermatophytosis is a disease of global significance caused by pathogenic keratinolytic fungi called dermatophytes in both animals and humans. Dermatophytes are broadly classified into three groups depending on their environmental habitat and include anthropophiles (living on humans), zoophiles (living on animals), and geophiles (living in the soil) [18]. Earlier all pathogenic dermatophytes were classified into three genera, namely *Microsporum*, *Trichophyton* and *Epidermophyton* [19].

This study aimed to extraction and quantification of *G. lucidum* triterpenoids, biological synthesis of ZnO nanoparticles from the aqueous extract of this mushroom, and evaluation the antifungal activity of these compounds against four dermatophytes isolated from Baghdad hospital.

MATERIALS AND METHODS

Pathogenic fungi collection

Dermatophytes were collected from Baghdad teaching hospital, Medical City, Baghdad, Iraq. The dermatophytes were isolated from different places of the skin and hairs by taking skin scrap using sterile glass slides. Hair specimens were collected by using sterile forceps to remove the hair from the root of the hair shaft. Scales were scratched from the surface utilizing sterile surgical blade. The dermatophytes were identified by direct microscopic examination using a drop of 10% of potassium hydroxide (KOH) heated (30 °C) for 5 minutes and was then allowed to cool down, then covered with a covers slip. Additionally, the specimens were cultured and spread directly on Sabouraud Dextrose Agar (SDA) and incubated at 28±2 °C for 10 days. Following the incubation period, positive cultures were analyzed both macroscopically and microscopically for species identification. The culture was classified as negative when the absence of a growth after the incubation period [20, 21].

Mushroom fruiting bodies

This study used Iraqi *G. lucidum* fruiting bodies obtained from National Center of Organic Farming, Ministry of Agriculture, Baghdad, Iraq. The fruiting bodies were dried at 45 °C for two days by using laboratory drier (Memmert, England). The dried fruiting bodies have been ground into powders using laboratory blender [22].

Production of Ganoderma lucidum Aqueous Extract (GLAE)

The dried fruiting bodies powders were extracted with hot water (1:20, w/v) at 75 °C for

2 hours in shaker water bath. The extraction was filtered by using gauze cloth then filter paper (Whatman no. 1). The GLAE was stored in a refrigerator until utilized for biosynthesis of ZnO nanoparticles [23].

Extraction of G. lucidum triterpenoids (GLTs)

The dried fruiting bodies powders were extracted with ethanol 70% (1:10, w/v) in a shaker at room temperature for 24 h. The extract was filtered firstly by gauze cloth then by Whatman filter paper number 1. The filtrate was evaporated to dryness at 35 °C under vacuum using a rotary evaporator (Heidolph, Germany) to produce concentrated ethanolic extract. The concentrated ethanolic extract was extracted with chloroform and water (1:1 v/v) three times. The chloroform layer was extracted with 5% saturated acquis $NaHCO_3$ three times. $NaHCO_3$ fraction was collected and acidified to pH 3-4 with 2N HCl under ice-cooling and re-extracted with chloroform. The chloroform was evaporated under rotary evaporator then transferred to small beaker to ensure evaporate all chloroform. The remaining mixture of acidic compounds referred to *Ganoderma lucidum* terpenoids (GLTs). This was stored in dark airtight container in a refrigerator until used for the experiment [24].

HPLC analysis of GLTs

HPLC model SYKAM (Germany) was used to analyses GLTs and detection of Ganoderic Acid by using (Ganoderic Acid A) as a standard (ChemFaces company, China. Purity >=98%). The mobile phase was ethanol : acetic acid 5% (40 : 60 v/v). The flow rate was 1.0 ml/min. Column was C18–ODS (25 cm * 4.6 mm). The injection volume was 0.1 ml. The detector UV-Vis was set at 243 nm [25].

Biosynthesis of ZnO nanoparticles

The biosynthesis procedure of ZnO nanoparticles was accomplished by using anhydrous zinc chloride ($ZnCl_2$) salt (Alfa Chemika, India). $ZnCl_2$ were mixed with the aqueous extraction of *G. lucidum* at a ratio (1:10 w/v), followed by placed the suspensions in a shaker at 150 rpm for 24 hours at dark conditions. After that, the suspensions were subjected to centrifugation at 6000 rpm for 15 minutes. The supernatants were discarded and the precipitates were collected and initially washed by of absolute ethanol then by deionized distilled water and centrifuge again. The resultant precipitates were collected and placed in an oven at 40 °C overnight. The resulting powders referred to ZnO nanoparticles which were collected and stored in a dark condition for further use [26, 27].

Characterization of ZnO nanoparticles

According to Alden, Yaaqoob [28], multiple techniques were employed to characterize the biosynthesized ZnO nanoparticles included:

UV spectrophotometer

UV spectrophotometer were used to detect the size and shape of nanoparticles in aqueous solution [29]. The samples were measured by UV spectrophotometer type (UV-9200. Biotech Engineering Management CO. LTD. UK) which were used to determine the optical absorption spectra of ZnO nanoparticles and *G. lucidum* aqueous extract.

Fourier transform infrared (FTIR)

The FTIR technique were utilized to identify the differences in the structures of biomolecules by detecting the differences in the functional groups. FTIR were conducted for the aqueous extract, $ZnCl_2$, ZnO nanoparticles, and $ZnCl_2$ with the aqueous extract together by using FTIR-8400 (Shimadzu, Japan) [30].

Atomic force microscopy (AFM)

AFM provide the 3D examination for ZnO nanoparticles as well as analyze the average size of these nanoparticles. AFM (Core-AFM 2023 model, manufactured by Nanosurf AG, Switzerland) were used to analyze the surface roughness and particle sizes of ZnO nanoparticles. The cantilever's force constant ranged from 28 to 75 nm. The probe specifications included a beam shape with a cantilever of 225 μm length and 38 μm width, and a frequency 190 kHz [29].

Energy dispersive X-ray spectroscopy (EDX)

EDX approach were employed to characterize the element distribution of ZnO nanoparticles and to provide the atomic and weight percentages of elements [26].

Field Emission Scanning Electron Microscope (FESEM)

FESEM is a technique that offer pictures of ZnO nanoparticles by sending an electron beam across

particles surface. This provide a high-resolution, 3D photographs of micrometer and nanometer sized particles. The dimension and shape of biosynthesized ZnO nanoparticles were examined utilizing Quattro S –STEM/SEM, Thermo Fisher Scientific, Czech Republic [31, 32].

Antifungal activity of ZnO nanoparticles and GLTs

Three concentrations from each of ZnO nanoparticles, GLTs, and ZnO with GLTs together were used to evaluate the antifungal activity of these compounds against four dermatophytes species. The concentrations were 25, 50, 100 mg/ml. The antifungal activity of these compounds were evaluated by plate diffusion method according to Hassan, Saadi [33] with some modifications.

Mycelial plugs with a 5 mm diameter were cut by cork borer from the growing margin of three days old cultures of dermatophytes species, transferred overhead to the center of fresh SDA petri dishes (9 cm in diameter) then incubated at 28 ± 2 °C for 3 days. After that, four holes were punched on the medium's surface for each dish utilizing a sterile cork borer (0.5 cm diameter), ensuring equal spacing between the holes. Subsequently, 70 µL were individually applied to each well. For control, sterile distilled water and DMSO were individually introduced into the wells of a separate dish. Fluconazole antifungal disc (10 µg) were used to compare the inhibition percentage among the tested compounds with Fluconazole. All dishes were incubated at 28 ± 2 °C for 7 days. After that, the mycelium colony diameter was measured using a digital ruler. Each treatment was consisted of three replicates.

The percentage of mycelia growth inhibition of dermatophytes species were measured and calculated after the incubation periods by using the formula:

Mycelia growth inhibition %= (G1 - G2) / G1 * 100 [34].

Where: G1 = The growth of dermatophytes species in petri dish with the holes contain distilled water and DMSO (control).

G2 = The growth of dermatophytes mycelia in petri dish with the holes contain the mentioned compounds.

RESULTS AND DISCUSSIONS

Pathogenic fungi collection

The patients were clinically diagnosed and mycological indicated to have tinea capitis (hair), tinea corporis (body ringworm), and tinea pedis (athlete's foot). From 70 obtained samples, 45 gave positive cultures and 25 gave negative cultures. Multiple dermatophytes were recognized based on macroscopic examination (surface and reverse color, topography, mycelial texture) and microscopic examination (two conidial types produced by dermatophytes: small unicellular microconidia and bigger septate macroconidia). From these positive samples, four dermatophytes were selected and used in this study which were the most frequent: *Microsporum canis, Trichophyton rubrum, Epidermophyton floccosum,* and *Trichophyton mentagrophytes.*

Extraction of GLTs

From the 1000 g of *G. lucidum* dried fruiting bodies powder which were used in this study, 16.1 g GLTs was extracted. This translates to 1.61% of the total powder. This result was in agreement with the study of [35] which extracted 1.67% of *G. lucidum* powder. However, this result was not agreed with the study of [24] which extracted 2.27% of GLTs from fruiting boding powder.

HPLC analysis of GLTs

The HPLC method was achieved by comparison of retention time for GLTs peaks with Ganoderic acid A standard. The results in the figure 1 showed the same peaks between the sample and the standard with the identical retention time (6.25 mins). The results showed that the concentration of Ganoderic acid in the sample was 985 µg per gram of the extract.

Biosynthesis of ZnO nanoparticles

ZnO nanoparticles were successfully biosynthesized using GLAE with $ZnCl_2$ salt. The biosynthesis of ZnO nanoparticles were confirmed by the optical examination. When combined $ZnCl_2$ with the aqueous extract modified the color of mixture to yellow indicating the synthesis of ZnO nanoparticles. After centrifugation and drying, a brownish-white powder was established. The modification in color confirmed the synthesis of ZnO back to the secondary metabolites which present in the aqueous extracts that act as a reducing agents [36]. This result agreed with the study of Abdullah, Jimenez-Rosado, Guerrero, Romero [37].

The green synthesis of ZnO nanoparticles is an uncomplicated procedure where a zinc salt such

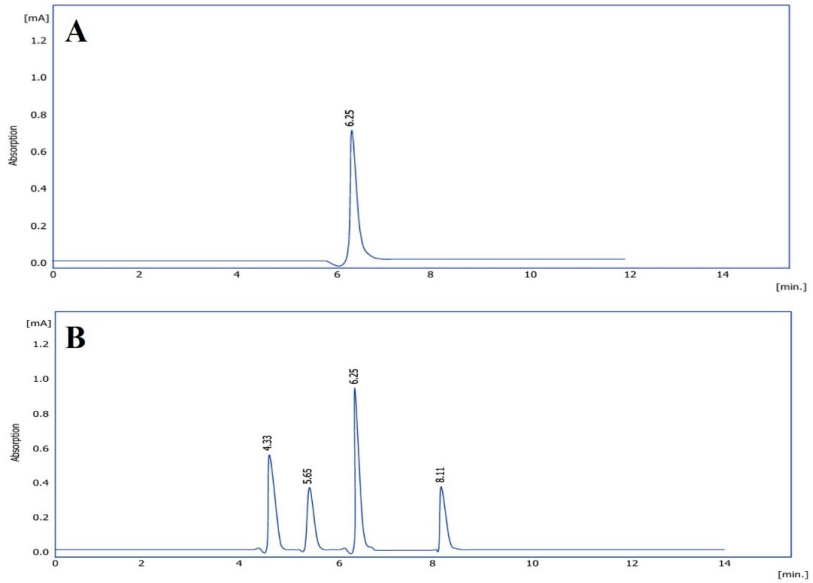

Fig. 1. HPLC chromatogram: (A): Ganoderic Acid A standard. (B): GLTs sample.

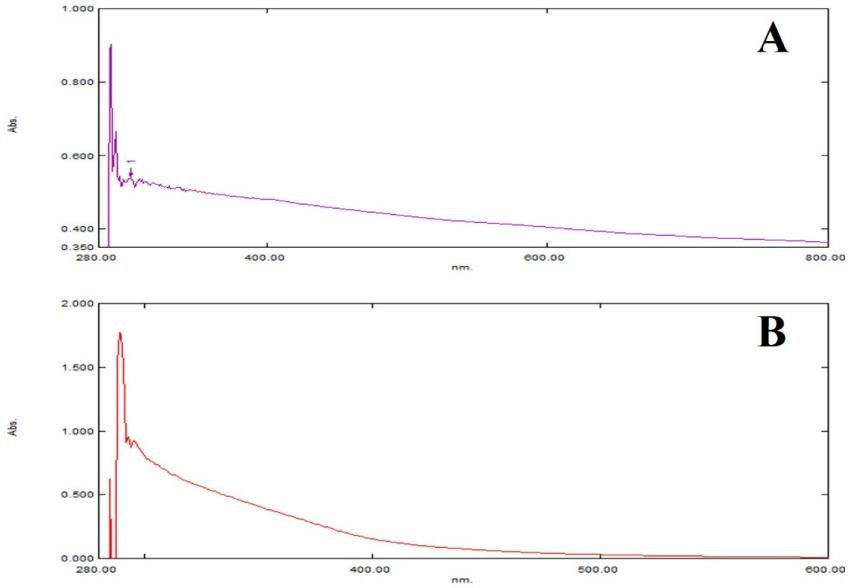

Fig. 2. UV spectrophotometer of ZnO nanoparticles and the GLAE, (A): ZnO, (B): GLAE.

as zinc nitrate or zinc chloride is supplied to the biological extract which lead to the preparation of ZnO nanoparticles [38]. The biological extracts containing secondary metabolites like terpenes, alkaloids, polysaccharides, flavonoids and others have the ability to the reduction and capping of Zn^{+2} ions in saline solutions. However, the oxidation process can yield stable and homogeneous distributed ZnO. The application of plant extracts in biosynthesis of ZnO nanoparticles support two primary roles: to facilitate the reduction of Zn^{+2} ions and to improve the stability of the resultant nanoparticles [39].

Characterization of ZnO nanoparticles

UV spectrophotometer

The absorption peaks of the biosynthesized ZnO nanoparticles and GLAE are shown in figure 2. Each of the samples demonstrate significant UV absorption, with absorption peaks range from 287

to 303 nm. After additional diluting by deionized distilled water of ZnO sample, the absorption peak was at 303 nm. This result corresponds to biosynthesized ZnO nanoparticles direct band emission. On the other hand, the absorption peak of the GLAE was at 289 nm. This result agreed with the study of Alden, Yaaqoob [28] which indicated that ZnO showed a UV absorption at 287 nm.

Fourier transform infrared (FTIR)

The biosynthesized ZnO nanoparticles were examined using FTIR spectroscopy at wavenumber between 4000 cm^{-1} and 400 cm^{-1} to identify the chemical bonds of ZnO and determine the phytochemicals in GLAE that responsible for stabilizing and capping the nanoparticles. Figure 3 demonstrate the FTIR spectrum of ZnO nanoparticles, GLAE and $ZnCl_2$

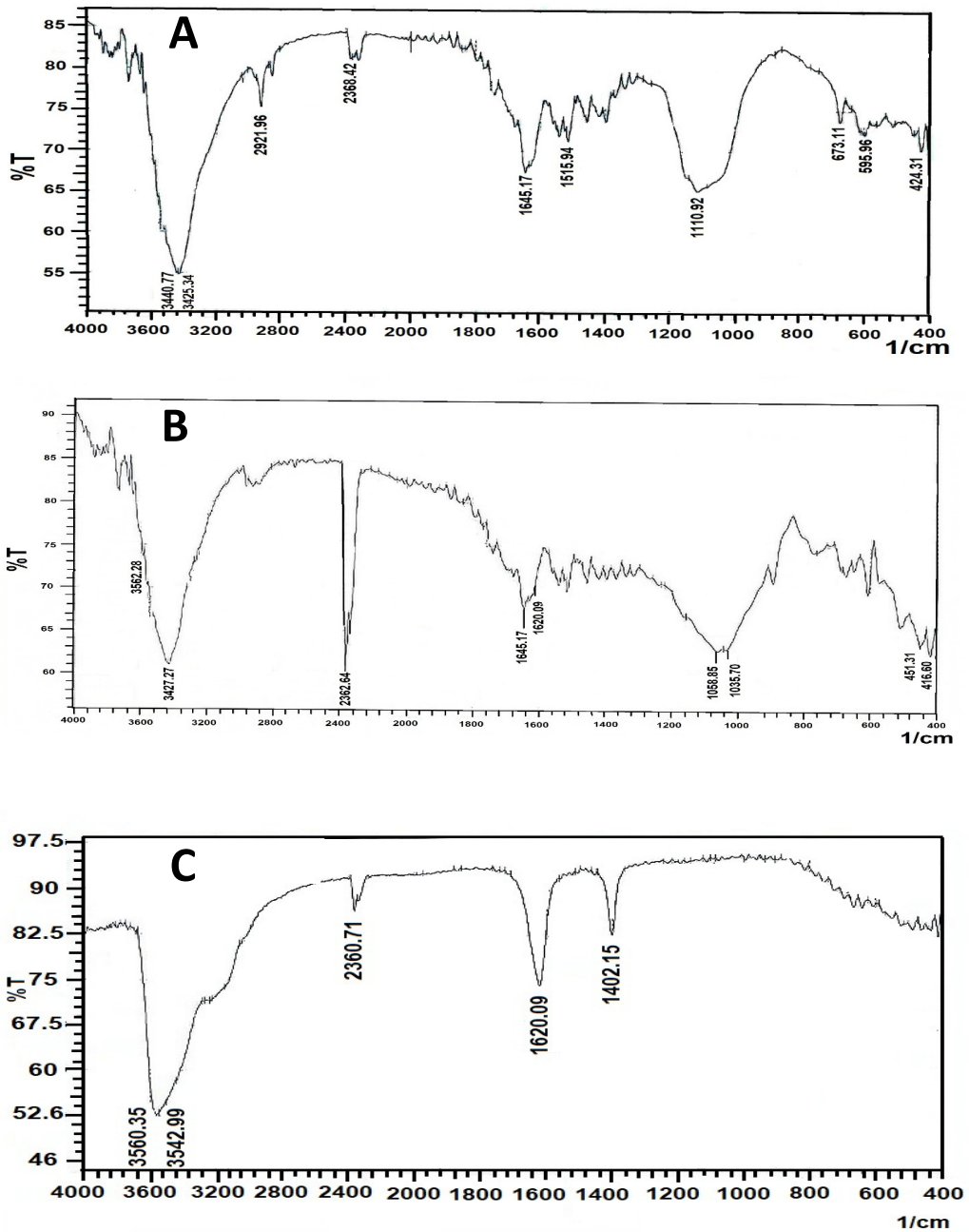

Fig. 3. FTIR results: (A): ZnO nanoparticles. (B): GLAE. (C): $ZnCl_2$.

salt. The highly peaks of ZnO nanoparticles situated at 3440.77 and 3425.34 cm^{-1} indicated the existence of -OH groups. Another peaks were denoted for ZnO at 2921.96, 2368.42, 1645.17, 1515.94, 1110.92, 673.11, 595.96. The ZnO stretching was at 424.31 cm^{-1}. The peaks of ZnO indicated the existence of O-H, C-H, and C-N stretching vibrations associated with aromatic and aliphatic amino groups. The FTIR of the aqueous extract has highly intense peak at 2362.64 cm^{-1} can be related to C=N stretch. The N-H bond Amine I groups are also observed at 1645.17 cm^{-1}. For zinc chloride salt, the FTIR result was 3560.35, 3542.99. 2360.71, 1620.09 and several peaks between 1402.15 and 432.03 cm^{-1}.

This result agreed with the study of Sanmugam, Vikraman, Venkatesan, Park [40] which produced a ZnO nanoparticles with chitosan, showing O-H stretching at around 3500 cm^{-1} and 1630 cm^{-1}, respectively. Additionally, the N-H deformation vibrations are seen at 1636 and 1562 cm^{-1}. The ZnO stretch appears at around 424 cm^{-1}.

Atomic force microscopy (AFM)

AFM was used to analyze the shape and size of ZnO nanoparticles in two and three- Dimensional view. Figure 4 show the 2D and 3D AFM images for ZnO nanoparticles. The 3D image of AFM showed a homogenous dispersion of ZnO with no visible agglomeration. The mean diameter of ZnO was 44.62 nm (figure 5). From this result,

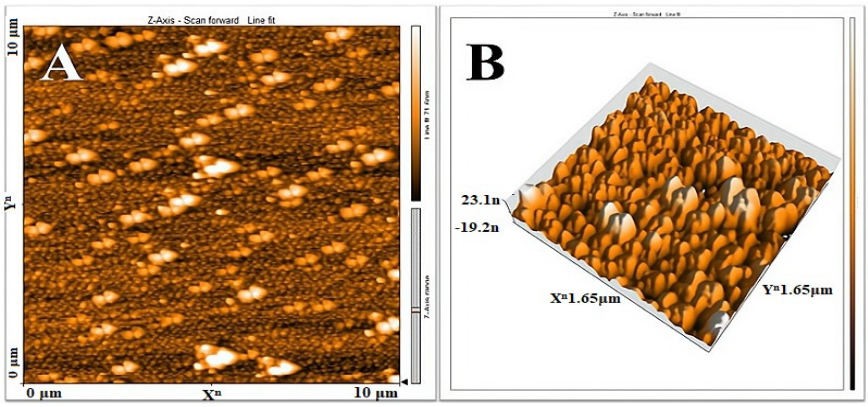

Fig. 4. AFM Analysis of the microscopic surface morphology of ZnO nanoparticles. (A): 2D view. (B): 3D view.

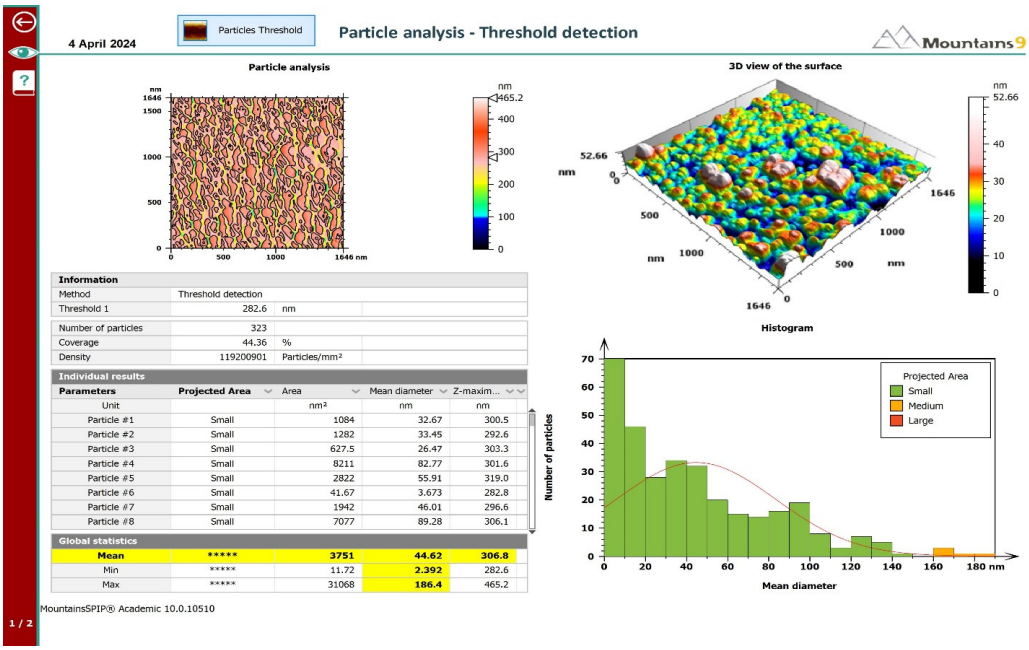

Fig. 5. Mean grain size of ZnO nanoparticles.

the extract may generate a particle capping, preventing material aggregation and maintaining the particulate size [41].

Energy dispersive X-ray spectroscopy (EDX)

The elemental analysis of ZnO nanoparticles was performed using EDX spectroscopy. The weight percentage of Zn element was 22% and for O was 45.9% (table 1). The EDX result of ZnO nanoparticles suggesting the existence of zinc and oxygen. ZnO nanoparticles exhibit distinctive high signal peaks at 1 keV and 8.5 keV for zinc, and a prominent peak at 0.5 keV for oxygen as shown in figure 6.

This result corresponds with the findings of [42] and [43] which indicated that Zn showed peaks at around 1 keV, 8.6 keV, and 9.5 keV. However, these findings indicated that O has a peak at about 0.5 Kev.

Field Emission Scanning Electron Microscope (FESEM)

The result of FESEM revealed that the particles formed were spherical, hexagonal, and triangular (figure 7). FESEM analysis indicated that the particle size ranges from 43.24 to 68.73 nm. This result significantly supports that GLAE could serve as a capping and reducing agent in the synthesis of ZnO nanoparticles.

Antifungal activity of Zn-NPs and GLTs.

Several studies evaluated the extractions and the bioactive compounds of *G. lucidum* against several fungal pathogens and demonstrating significant antimicrobial activity. Nevertheless, there are only a few works that have been reported about the antidermatophytes efficacy of this mushroom. Hence, one of the primary objectives of this study was to evaluate the antidermatophytic efficacy of the *G. lucidum* triterpenoids with zinc oxide nanoparticles synthesized from the aqueous extract of this mushroom against four dermatophytes isolated from Baghdad Hospital. The plates diffusion method was evaluated to distinguish between the activity of ZnO nanoparticles, triterpenoids extraction and the mixture between them against

Table 1. The percentage of atomic and weight of elements in EDX analysis

Elements	Atomic %	Weight %
C	3.2	12.2
N	8.2	6.6
O	49.8	45.9
Zn	31.8	22.0
Al	0.8	1.2
Si	0.7	1.1
P	1.9	3.4
S	0.7	1.4
Cl	1.4	2.8
Ca	1.5	3.4

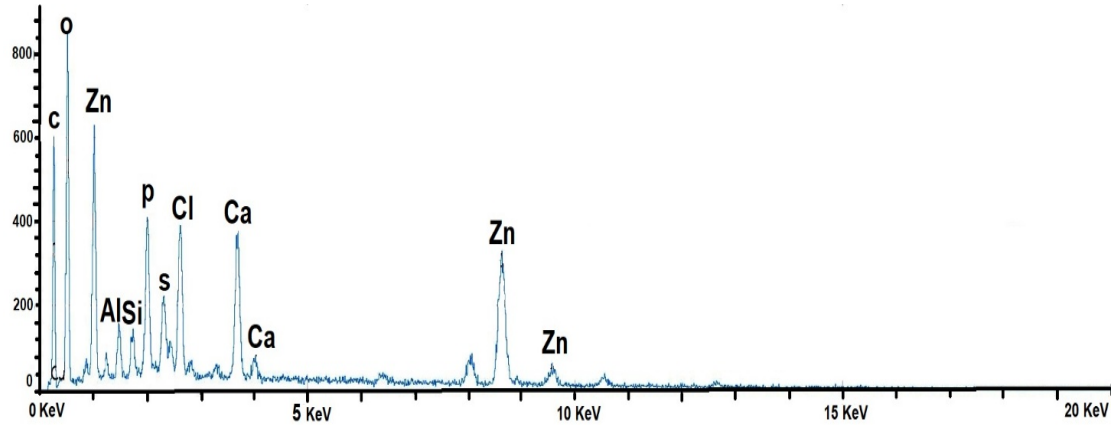

Fig. 6. EDX image of the biosynthesized ZnO nanoparticles

four dermatophytes by calculating the percentage of inhibition of mycelia growth after the incubation at 28 ± 2 °C for 7 days. Three concentrations were used from each treatment to assess the antifungal activity compared with Fluconazole antifungal (10 µg) and control treatment (DMSO or D.W). It can be seen from the data in table 2, 3, 4, and 5 there was a significant difference among treatments for

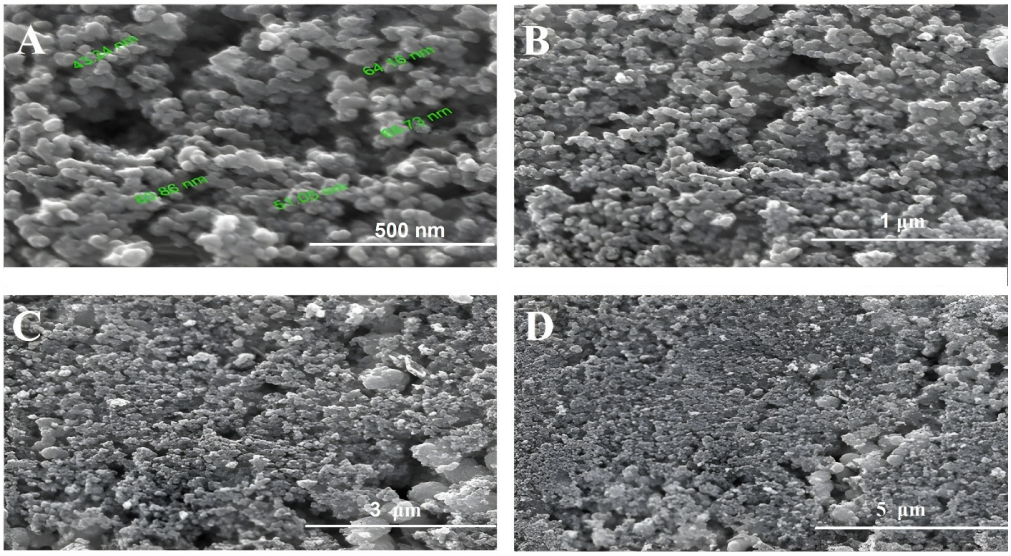

Fig. 7. FESEM images at different magnification of the biosynthesized ZnO nanoparticles, (A): x120000. (B): x60000. (C): x30000. (D): x15000

Table 2. The efficacy of three concentrations of ZnO, GLTs, and ZnO with GLTs against *M. canis* after 7 days of incubation at 28 ± 2 °C.

Treatments	The inhibition percentage %			Mean of Treatment
	25 mg/ml	50 mg/ml	100 mg/ml	
ZnO	26.230	28.830	34.030	29.697
GLTs	22.930	25.870	33.670	27.490
ZnO +GLTs (1:1)	48.870	55.500	59.970	54.780
Fluconazole	65.130	65.130	65.130	65.130
Control	0.000	0.000	0.000	0.000
L S D (P=0.05)	Treatment	Concentration		Interaction
	1.797**	1.177**		3.113**

Table 3. The efficacy of three concentrations of ZnO, GLTs, and ZnO with GLTs against *T. rubrum* after 7 days of incubation at 28 ± 2 °C.

Treatments	The inhibition percentage %			Mean of Treatment
	25 mg/ml	50 mg/ml	100 mg/ml	
ZnO	39.570	47.370	59.970	48.970
GLTs	26.600	35.500	46.230	36.110
ZnO +GLTs	56.600	61.470	66.600	61.557
Fluconazole	65.870	65.870	65.870	65.870
Control	0.000	0.000	0.000	0.000
L S D (P=0.05)	Treatment	concentration		interaction
	1.394**	0.913**		2.415**

Table 4. The efficacy of three concentrations of ZnO, GLTs, and ZnO with GLTs against *E. floccosum* after 7 days of incubation at 28 ± 2 °C.

Treatments	The inhibition percentage %			Mean of Treatment
	25 mg/ml	50 mg/ml	100 mg/ml	
ZnO	28.470	35.870	40.370	34.903
GLTs	38.070	42.570	45.500	42.047
ZnO +GLTs	50.730	55.500	62.530	56.253
Fluconazole	68.470	68.470	68.470	68.470
Control	0.000	0.000	0.000	0.000
L S D (P=0.05)	Treatment	concentration		interaction
	1.900**	1.244**		3.291**

Table 5. The efficacy of three concentrations of ZnO, GLTs, and ZnO with GLTs against *T. mentagrophytes* after 7 days of incubation at 28 ± 2 °C.

Treatment	**The inhibition percentage %**			**Mean of Treatment**
	25 mg/ml	50 mg/ml	100 mg/ml	
ZnO	27.000	34.770	41.470	34.413
GLTs	28.470	34.400	41.830	34.900
ZnO +GLTs	44.400	54.400	59.230	52.677
Fluconazole	60.330	60.330	60.330	60.330
Control	0.000	0.000	0.000	0.000
L S D (P=0.05)	Treatment	concentration		interaction
	2.175**	1.424**		3.767**

inhibit the four dermatophytes. The combinations between the biosynthesized ZnO nanoparticles with GLTs showed synergistic effect to inhibit the growth of *M. canis*, *T. rubrum*, *E. floccosum*, and *T. mentagrophytes*. The concentration 100 mg/ml of this treatment showed highest inhibition percentage followed by 50 and 25 mg/ml on the above dermatophytes. In other words, the inhibition percentage increased by increasing the concentrations of the tested treatments (figure 8, 9, 10, and 11).

The expense and side effects of the antifungal drugs with the resistance of fungi and the prolong treatment of dermatophyte diseases required alternate treatments that both safe and effective [44]. *G lucidum* was utilized for hundreds of years in traditional medicine for medical treatment and the improvement of general well-being [45]. *G. lucidum* is a rich source of unique chemicals and exhibits several properties, including antifungal effects. It also contains many biologically active compounds that showed activity against different pathogenic fungus [46]. However, there are limited studies on the extractions of *G. lucidum* fruiting bodies antimicrobial efficacy against human infections, especially dermatophytes [16]. The antifungal properties of *G. lucidum* are linked to the presence of ganoduric protein. The capacity of phytochemicals in *G. lucidum* extracts to pass through cellular membranes, cell walls, and cytoplasmic components of pathogenic fungi may result in the suppression of these human fungal diseases [44, 47]. On the other hand, ZnO nanoparticles have demonstrated antidermatophytic action. The antifungal mechanism is mainly associated with the production of extremely reactive ions or substances, like OH-, H_2O_2, or O_2, with the ability to destroy the fungal cell wall or plasma membrane [15]. The antimicrobial activity of metallic nanoparticles remains a subject of ongoing discussion in various aspects. According to scientific reports, the primary mechanisms identified include the generation of reactive oxidative species (ROS) and the removal of metal ions from nanoparticles resulting from their interaction with the cell membrane. This interaction leads to the inhibition of cell wall synthesis, disruption of enzyme activities, cell signaling,

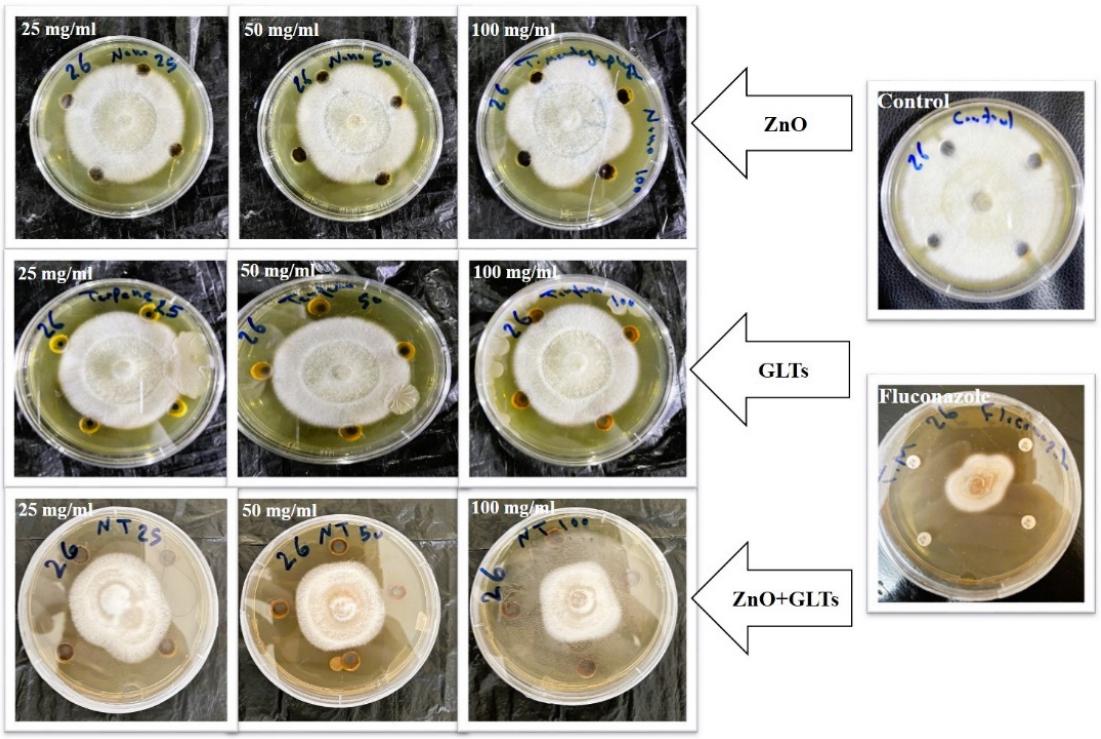

Fig. 8. The efficacy of three concentrations of ZnO, GLTs, and ZnO with GLTs against *T. mentagrophytes* after 7 days of incubation at 28 ± 2 °C.

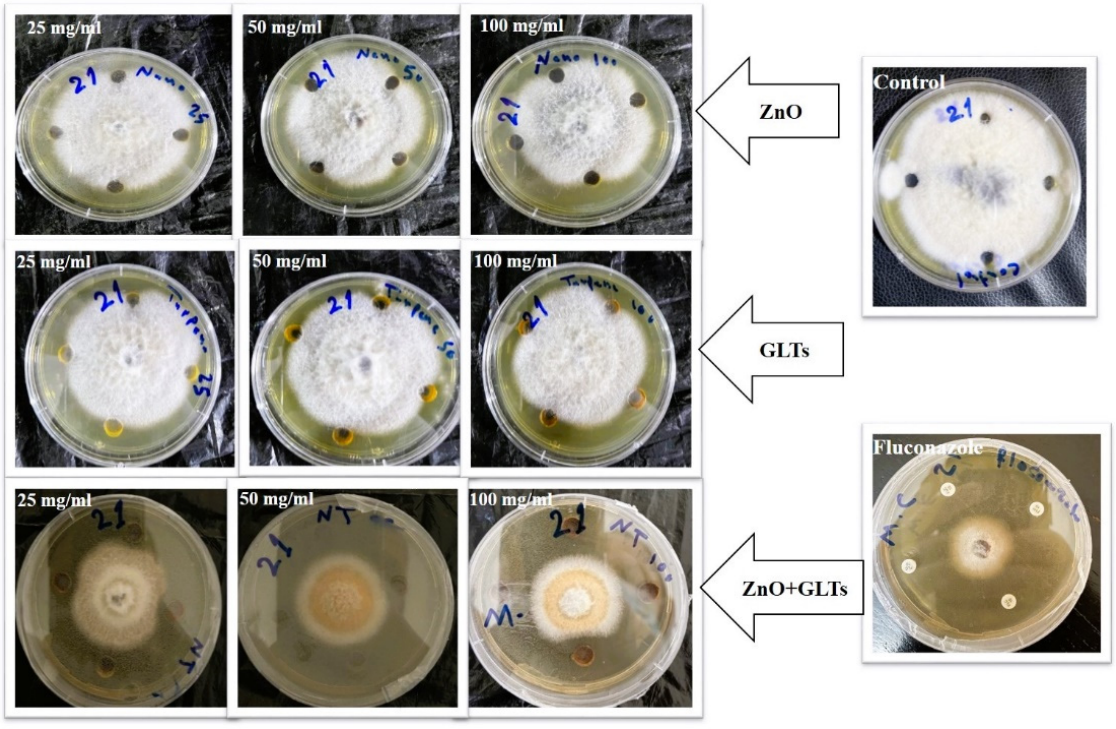

Fig. 9. The efficacy of three concentrations of ZnO, GLTs, and ZnO with GLTs against *M. canis* after 7 days of incubation at 28 ± 2 °C.

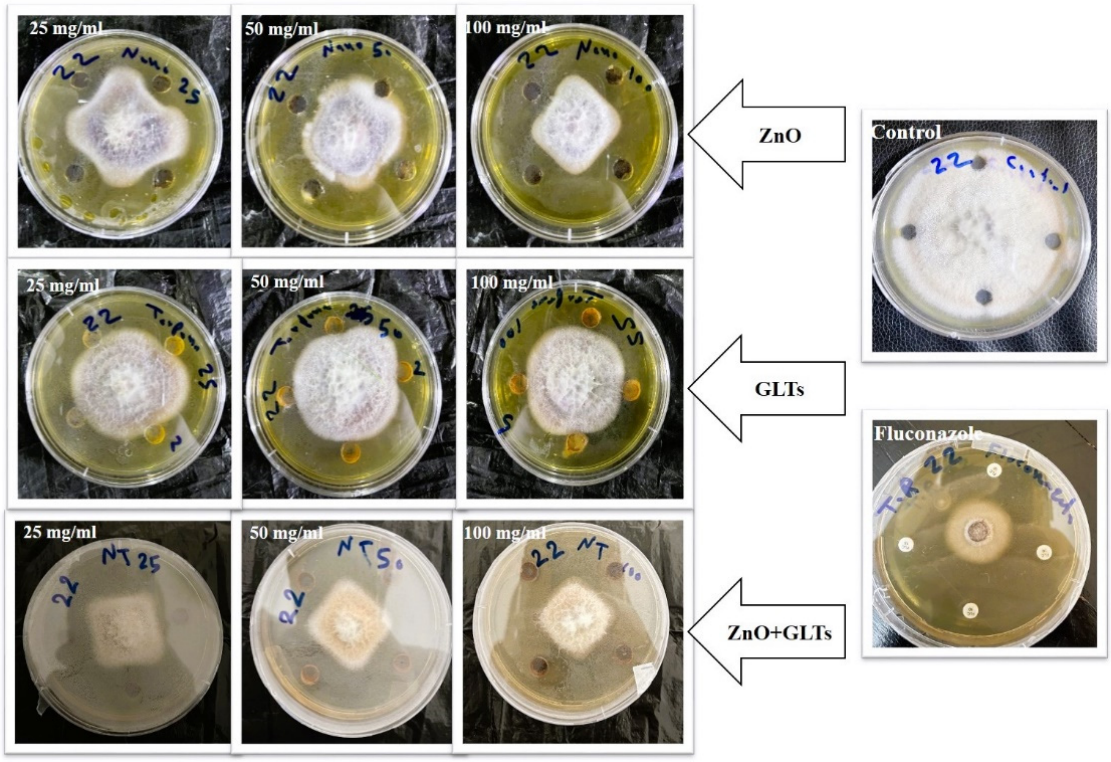

Fig. 10. The efficacy of three concentrations of ZnO, GLTs, and ZnO with GLTs against *T. rubrum* after 7 days of incubation at 28 ± 2 °C.

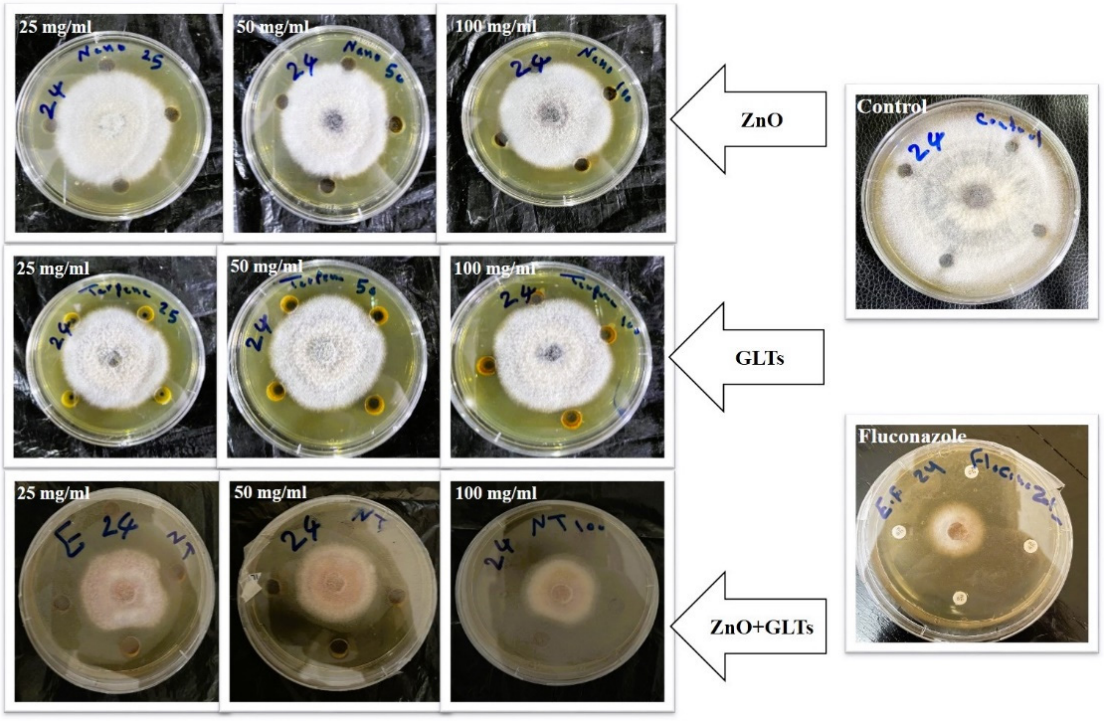

Fig. 11. The efficacy of three concentrations of ZnO, GLTs, and ZnO with GLTs against *E. floccosum* after 7 days of incubation at 28 ± 2 °C.

DNA damage, ribosome disassembly, deactivation of protein synthesis, and alterations in the structure of essential proteins. The accumulation of positively charged Zn^{+2} from the dissolving of ZnO nanoparticles leads to membrane dysfunction, while the absorption of ZnO nanoparticles interferes with microbial metabolic activity leading to microbial cell death [48, 49]. In most fungi, the primary component of the cell wall is a branching β-1,3; β-1,6 glucan, which is connected to chitin through a β-1,4 linkage. The binding of oxide particles to the fungal cell surface by electrostatic interactions may constitute a primary mechanism [50]. Consequently, the combination of ZnO and GLTs can enhance the antifungal efficacy of each chemical by increasing the inhibitory percentage against each dermatophyte.

CONCLUSION

Ganoderma lucidum is one of the most important medicinal mushroom which were used in traditional Chinese medicine due to has several active ingredients. GLTs were successfully extracted and identified from this medicinal mushroom. ZnO nanoparticles were successfully biosynthesized by using the aqueous extract of *G. lucidum* and were characterized by using several approaches. The GLTs along with ZnO nanoparticles showed higher antidermatophytic activity. Each of GLTs and ZnO nanoparticles have antifungal effect against all tested dermatophytes. However, the combination of GLTs with ZnO showed synergistic effect at all concentrations and the inhibition percentage increased with increasing the concentrations. This study recommends to use the combination between GLTs and ZnO nanoparticles against other systematic fungal pathogens.

FUNDING

No funding has been received to complete this study.

CONFLICT OF INTEREST

The authors declare that there are no conflicts of interest.

ACKNOLEDGEMENTS

The authors would like to thank the staff of Department of Biology, College of Science, University of Baghdad. In addition, the authors want to acknowledge the National Center of Organic Farming, Iraqi Ministry of Agriculture.

REFERENCES

1. Gonzalez A, Atienza V, Montoro A, Soriano JM. Use of Ganoderma lucidum (Ganodermataceae, Basidiomycota) as Radioprotector. Nutrients, 2020;12 (4):1143. https://doi.org/10.3390/nu12041143
2. Commission CP. Chinese pharmacopoeia. China Medical Science Press: Beijing, China, 2015;1:191-193.
3. Sheng F, Wang S, Luo X, Xiao J, Hu L, Li P. Simultaneous determination of ten nucleosides and bases in Ganoderma by micellar electrokinetic chromatography. Food Science and Human Wellness, 2022;11 (2):263-268. https://doi.org/10.1016/j.fshw.2021.11.015
4. Li C, Cui Y, Lu J, Liu C, Chen S, Ma C, Liu Z, Wang J, Kang W. Ionic Liquid-Based Ultrasonic-Assisted Extraction Coupled with HPLC and Artificial Neural Network Analysis for Ganoderma lucidum. Molecules, 2020;25 (6):1309. https://doi.org/10.3390/molecules25061309
5. Zheng W, Lan S, Zhang W, Nie B, Zhu K, Ye X, Hou Z, Chen S. Polysaccharide structure evaluation of Ganoderma lucidum from different regions in China based on an innovative extraction strategy. Carbohydr Polym, 2024;335:122079. https://doi.org/10.1016/j.carbpol.2024.122079
6. Liu J, Kurashiki K, Fukuta A, Kaneko S, Suimi Y, Shimizu K, Kondo R. Quantitative determination of the representative triterpenoids in the extracts of Ganoderma lucidum with different growth stages using high-performance liquid chromatography for evaluation of their 5α-reductase inhibitory properties. Food Chemistry, 2012;133 (3):1034-1038. https://doi.org/10.1016/j.foodchem.2012.01.034
7. Cilerdzic JL, Sofrenic IV, Tesevic VV, Brceski ID, Duletic-Lausevic SN, Vukojevic JB, Stajic MM. Neuroprotective Potential and Chemical Profile of Alternatively Cultivated Ganoderma lucidum Basidiocarps. Chemistry & Biodiversity, 2018;15 (5):e1800036. https://doi.org/10.1002/cbdv.201800036
8. Roy A, Bulut O, Some S, Mandal AK, Yilmaz MD. Green synthesis of silver nanoparticles: biomolecule-nanoparticle organizations targeting antimicrobial activity. RSC Adv, 2019;9 (5):2673-2702. https://doi.org/10.1039/C8RA08982E
9. Mohammed GM, Hawar SN. Green Biosynthesis of Silver Nanoparticles from Moringa oleifera Leaves and Its Antimicrobial and Cytotoxicity Activities. Int J Biomater, 2022;2022 (1):4136641. https://doi.org/10.1155/2022/4136641
10. Humud H, Al-Kafiji T, Al-araji A, Ali L. Au-Ag-Cu nanoparticles alloys showed antifangal activity against the antibiotics-resistant Candida albicans. IOP Conference Series: Materials Science and Engineering. Vol 757: IOP Publishing; 2020:012049. https://doi.org/10.1088/1757-899X/757/1/012049
11. Sajid M, Płotka-Wasylka J. Nanoparticles: Synthesis, characteristics, and applications in analytical and other sciences. Microchemical Journal, 2020;154:104623. https://doi.org/10.1016/j.microc.2020.104623
12. Gour A, Jain NK. Advances in green synthesis of nanoparticles. Artif Cells Nanomed Biotechnol, 2019;47 (1):844-851. https://doi.org/10.1080/21691401.2019.1577878
13. Ijaz I, Gilani E, Nazir A, Bukhari A. Detail review on chemical, physical and green synthesis, classification, characterizations and applications of nanoparticles. Green

Chemistry Letters and Reviews, 2020;13 (3):223-245. https://doi.org/10.1080/17518253.2020.1802517
14. Khan ZUH, Sadiq HM, Shah NS, Khan AU, Muhammad N, Hassan SU, Tahir K, Safi SZ, Khan FU, Imran M, Ahmad N, Ullah F, Ahmad A, Sayed M, Khalid MS, Qaisrani SA, Ali M, Zakir A. Greener synthesis of zinc oxide nanoparticles using Trianthema portulacastrum extract and evaluation of its photocatalytic and biological applications. J Photochem Photobiol B, 2019;192:147-157. https://doi.org/10.1016/j.jphotobiol.2019.01.013
15. Al-Janabi AAHS, Bashi AM. Synthesis and antifungal activity of novel griseofulvin nanoparticles with zinc oxide against dermatophytic fungi: Trichophyton mentagrophytes and Trichophyton verrucosum: A primary study. Current Medical Mycology, 2022;8 (2):40.
16. Erbiai EH, Amina B, Kaoutar A, Saidi R, Lamrani Z, Pinto E, Esteves da Silva JCG, Maouni A, Pinto da Silva L. Chemical Characterization and Evaluation of Antimicrobial Properties of the Wild Medicinal Mushroom Ganoderma lucidum Growing in Northern Moroccan Forests. Life (Basel), 2023;13 (5):1217. https://doi.org/10.3390/life13051217
17. Weitzman I, Summerbell RC. The dermatophytes. Clinical Microbiology Reviews, 1995;8 (2):240-259. https://doi.org/10.1128/CMR.8.2.240
18. Baert F, Stubbe D, D'Hooge E, Packeu A, Hendrickx M. Updating the Taxonomy of Dermatophytes of the BCCM/IHEM Collection According to the New Standard: A Phylogenetic Approach. Mycopathologia, 2020;185 (1):161-168. https://doi.org/10.1007/s11046-019-00338-7
19. de Hoog GS, Dukik K, Monod M, Packeu A, Stubbe D, Hendrickx M, Kupsch C, Stielow JB, Freeke J, Goker M, Rezaei-Matehkolaei A, Mirhendi H, Graser Y. Toward a Novel Multilocus Phylogenetic Taxonomy for the Dermatophytes. Mycopathologia, 2017;182 (1-2):5-31. https://doi.org/10.1007/s11046-016-0073-9
20. Shalaby MF, El-Din AN, El-Hamd MA. Isolation, Identification, and In Vitro Antifungal Susceptibility Testing of Dermatophytes from Clinical Samples at Sohag University Hospital in Egypt. Electron Physician, 2016;8 (6):2557-2567. https://doi.org/10.19082/2557
21. Assi SR, Al-Aaraji AM. Antifungal Activity of Trichoderma orientale FMR 12486 Crude Extract against Some Human Pathogenic Fungi. Iraqi Journal of Science, 2024:1250-1265. https://doi.org/10.24996/ijs.2024.65.3.7
22. Vu D. Effects of extraction solvents on phytochemicals and bioactivities of Ganoderma lucidum. Egyptian Journal of Chemistry, 2023;66 (9):581-588. https://doi.org/10.21608/ejchem.2023.172356.7142
23. Smirnov O, Dzhagan V, Kovalenko M, Gudymenko O, Dzhagan V, Mazur N, Isaieva O, Maksimenko Z, Kondratenko S, Skoryk M, Yukhymchuk V. ZnO and Ag NP-decorated ZnO nanoflowers: green synthesis using Ganoderma lucidum aqueous extract and characterization. RSC Adv, 2022;13 (1):756-763. https://doi.org/10.1039/D2RA05834K
24. Oluba OM. Ganoderma terpenoid extract exhibited anti-plasmodial activity by a mechanism involving reduction in erythrocyte and hepatic lipids in Plasmodium berghei infected mice. Lipids Health Dis, 2019;18 (1):12. https://doi.org/10.1186/s12944-018-0951-x
25. Chen D-H, Wang J-Y, Chen M-T, Liu Y-C, Chen K-D. The Triterpenoid High-Performance Liquid Chromatography Analytical Profiles of the Mycelia of Ganoderma lucidum (lingzhi). Microbiology Research, 2023;14 (3):1353-1363. https://doi.org/10.3390/microbiolres14030092
26. Ranjith Santhosh Kumar D, Elango N, Selvaraju GD, Matthew PA, Palanisamy S, Cho H, Al Khattaf FS, Hatamleh AA, Roy AD. Mycosynthesis of zinc oxide nanoparticles coated with silver using Ganoderma lucidum (Curtis) P. Karst and its evaluation of in vitro antidiabetic and anticancer potential. Journal of Nanomaterials, 2022;2022 (1):2798532. https://doi.org/10.1155/2022/2798532
27. Can A, Kizilbey K. Green Synthesis of ZnO Nanoparticles via Ganoderma Lucidum Extract: Structural and Functional Analysis in Polymer Composites. Gels, 2024;10 (9):576. https://doi.org/10.3390/gels10090576
28. Alden MA, Yaaqoob L. Evaluation of the Biological Effect Synthesized Zinc Oxide Nanoparticles on Pseudomonas aeruginosa. Iraqi Journal of Agricultural Sciences, 2022;53 (1):27-37. https://doi.org/10.36103/ijas.v53i1.1502
29. Tamkeen RM, Al-Bahrani RM. Treatment isolated fungi from laboratory tools in some Baghdad hospitals by using biosynthesized nanoparticles. Iraqi Journal of Science, 2019:1673-1681. https://doi.org/10.24996/ijs.2019.60.8.3
30. Mandal AK, Katuwal S, Tettey F, Gupta A, Bhattarai S, Jaisi S, Bhandari DP, Shah AK, Bhattarai N, Parajuli N. Current Research on Zinc Oxide Nanoparticles: Synthesis, Characterization, and Biomedical Applications. Nanomaterials (Basel), 2022;12 (17):3066. https://doi.org/10.3390/nano12173066
31. Jayachandran A, T RA, Nair AS. Green synthesis and characterization of zinc oxide nanoparticles using Cayratia pedata leaf extract. Biochem Biophys Rep, 2021;26:100995. https://doi.org/10.1016/j.bbrep.2021.100995
32. Nakamae K. Electron microscopy in semiconductor inspection. Measurement Science and Technology, 2021;32 (5):052003. https://doi.org/10.1088/1361-6501/abd96d
33. Hassan AA, Saadi MA. Isolation, Identification and Cultivation of Ganoderma spp. and Evaluation of Their Efficiency in Inhibiting Plant Pathogenic Fungi Fusarium oxysporum and Alternaria tenuissima. IOP Conference Series: Earth and Environmental Science. Vol 1158: IOP Publishing; 2023:072021. https://doi.org/10.1088/1755-1315/1158/7/072021
34. Intana W, Chamswarng C, Intanoo W, Hongprayoon C, Sivasithamparam K. Use of mutant strains for improved efficacy of Trichoderma harzianum for controlling cucumber damping-off. Thai Journal of Agricultural Science, 2003;36:429-439.
35. Gao Y, Zhang R, Zhang J, Gao S, Gao W, Zhang H, Wang H, Han B. Study of the extraction process and in vivo inhibitory effect of ganoderma triterpenes in oral mucosa cancer. Molecules, 2011;16 (7):5315-5332. https://doi.org/10.3390/molecules16075315
36. Nawar MH, Yaaqoob LA, Hatem MW, Mohammed AK. The effect of nanoparticles preparation from extract of Dodonaea Viscosa L. leaves on the biological performance of the Great Waxworm. AIP Conference Proceedings . AIP Publishing. Vol 2922: AIP Publishing; 2024. https://doi.org/10.1063/5.0183841
37. Abdullah JAA, Jimenez-Rosado M, Guerrero A, Romero A. Biopolymer-Based Films Reinforced with Green Synthesized Zinc Oxide Nanoparticles. Polymers (Basel), 2022;14 (23):5202. https://doi.org/10.3390/polym14235202
38. Xu J, Huang Y, Zhu S, Abbes N, Jing X, Zhang L. A

review of the green synthesis of ZnO nanoparticles using plant extracts and their prospects for application in antibacterial textiles. Journal of Engineered Fibers and Fabrics, 2021;16:15589250211046242. https://doi.org/10.1177/15589250211046242

39. Zeghoud S, Hemmami H, Seghir BB, Amor IB, Kouadri I, Rebiai A, Messaoudi M, Ahmed S, Pohl P, Simal-Gandara J. A review on biogenic green synthesis of ZnO nanoparticles by plant biomass and their applications. Materials Today Communications, 2022;33:104747. https://doi.org/10.1016/j.mtcomm.2022.104747
40. Sanmugam A, Vikraman D, Venkatesan S, Park HJ. Optical and Structural Properties of Solvent Free Synthesized Starch/Chitosan-ZnO Nanocomposites. Journal of Nanomaterials, 2017;2017 (1):1-8. https://doi.org/10.1155/2017/7536364
41. Mazhir SN, Abdalameer NK, Yaaqoob LA, Hammood JK. Cold plasma synthesis of Zinc Selenide Nanoparticles for inhibition bacteria using disc diffusion. Physics and Chemistry of Solid State, 2022;23 (4):652-658. https://doi.org/10.15330/pcss.23.4.652-658
42. Radhakrishnan AK, Nair S, Santhanagopalan D. N-doped carbon nanosheets as high-performance anodes for Li- and Na-ion batteries. Journal of Materials Research, 2019;35 (1):12-19. https://doi.org/10.1557/jmr.2019.330
43. Agarwal H, Menon S, Shanmugam VK. Functionalization of zinc oxide nanoparticles using Mucuna pruriens and its antibacterial activity. Surfaces and Interfaces, 2020;19:100521. https://doi.org/10.1016/j.surfin.2020.100521
44. Ogidi OC, Oyetayo VO. Phytochemical property and assessment of antidermatophytic activity of some selected wild macrofungi against pathogenic dermatophytes. Mycology, 2016;7 (1):9-14. https://doi.org/10.1080/21501203.2016.1145608
45. Reddy EP. Phytochemical Analysis and Antifungal Activity of Ganoderma lucidum. Indian Journal of Public Health Research & Development, 2018;9 (12). https://doi.org/10.5958/0976-5506.2018.01820.X
46. Saludares G, Amper C, Lituanas I. Antimicrobial performances of Ganoderma lucidum extract against fruits and leaves pathogens. IOP Conference Series: Earth and Environmental Science. Vol 1145: IOP Publishing; 2023:012019. https://doi.org/10.1088/1755-1315/1145/1/012019
47. Wang H, Ng TB. Ganodermin, an antifungal protein from fruiting bodies of the medicinal mushroom Ganoderma lucidum. Peptides, 2006;27 (1):27-30. https://doi.org/10.1016/j.peptides.2005.06.009
48. Gharpure S, Yadwade R, Ankamwar B. Non-antimicrobial and Non-anticancer Properties of ZnO Nanoparticles Biosynthesized Using Different Plant Parts of Bixa orellana. ACS Omega, 2022;7 (2):1914-1933. https://doi.org/10.1021/acsomega.1c05324
49. Djearamane S, Xiu L-J, Wong L-S, Rajamani R, Bharathi D, Kayarohanam S, De Cruz AE, Tey L-H, Janakiraman AK, Aminuzzaman M. Antifungal properties of zinc oxide nanoparticles on Candida albicans. Coatings, 2022;12 (12):1864. https://doi.org/10.3390/coatings12121864
50. El-Diasty EM, Ahmed M, Okasha N, Mansour SF, El-Dek SI, El-Khalek H, Youssif MH. Antifungal activity of zinc oxide nanoparticles against dermatophytic lesions of cattle. Rom J Biophys, 2013;23 (3):191-202.